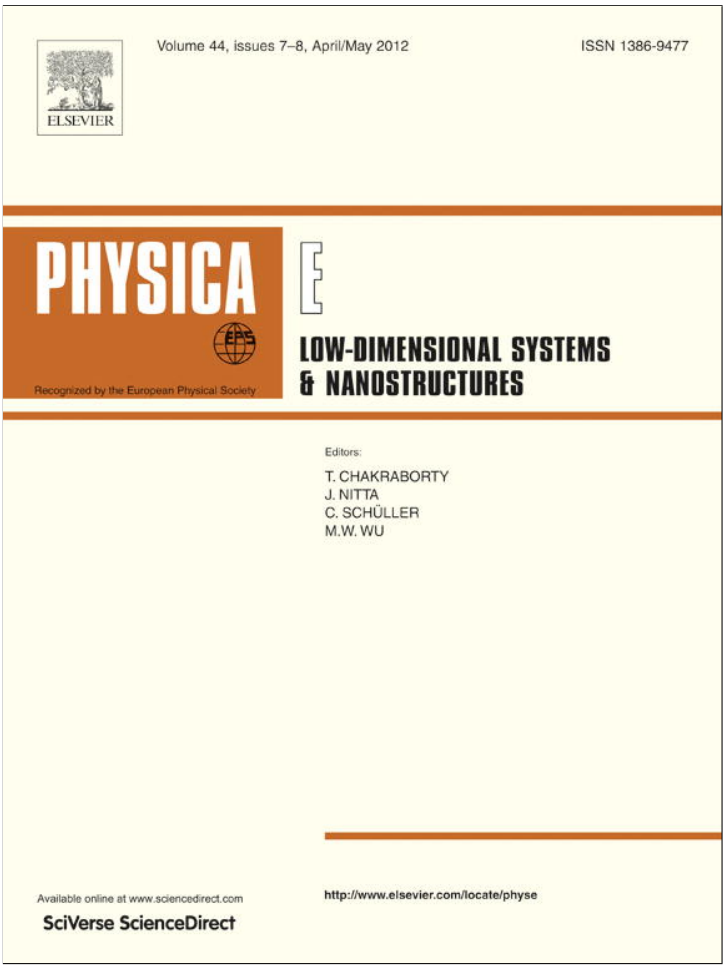

Physica E 44 (2012) 1528–1534

Contents lists available at SciVerse ScienceDirect

Physica E

journal homepage: www.elsevier.com/locate/physe

Zeptogram sensing from gigahertz vibration: Graphene based nanosensor

S. Adhikari, R. Chowdhury *

Multidisciplinary Nanotechnology Centre, Swansea University, Singleton Park, Swansea SA2 8PP, UK

ARTICLE INFO

Article history:
Received 27 January 2012
Accepted 16 March 2012
Available online 29 March 2012

ABSTRACT

We develop the mathematical framework for using single layer graphene sheet as nanoscale label-free mass sensors. Graphene resonators are assumed to be in the cantilevered configuration. Four types of mass loadings are considered and closed-form equations are derived for the frequency shift due to the added mass. Using the potential and kinetic energy of the mass loaded graphene sheets, generalised non-dimensional calibration constants are proposed for an explicit relationship between the added mass and the frequency shift. These equations in turn are used for sensing the added mass. Numerical results illustrate that the sensitivity of graphene sensors is in the order of gigahertz/zeptogram. We show that the performance of the sensor depends on the spatial distribution of the attached mass on the graphene sheet.

1. Introduction

In today's world there exist various kinds of threats originating from different household as well as industrial applications. Many of these threats are in the form of gases, chemicals and bio-fragments. In this context, effective detection systems or sensors are required. Sensing of biological objects is also useful for drug-delivery. The best sensors would be the ones which are able to detect small number of molecules/atoms of the gas and chemicals which needs to be detected [1,2] with least amount of change in some measured quantity. Among the various types of sensors, solid state sensors have received significant attention. These sensors include solid electrolyte sensors [3], catalytic sensors [4], bio sensor [5] and semiconducting oxide gas sensors [6–9].

New class of sensors were developed following the discovery of fullerene and carbon nanotube (CNT). Electronic sensors made of fullerene were very sensitive to any adsorbed molecule. Electron transport through CNT is influenced by the functionalisation of side walls and therefore, by controlling the defect sites one can enhance the sensitivity of the sensor. However, the recent discovery of graphene [10,11] has opened completely new area that promises ultra-sensitive and ultra-fast electronic sensor due to low electrical noise material. Graphene is made up of a single layer of carbon atoms packed into a two-dimensional honeycomb lattice. It has attracted tremendous attention in both its 2D and 1D forms, the latter being obtained by patterning the layer into strip or ribbon. Scanning probe microscopy of graphene ribbons [12] revealed bright stripes along its edges, suggesting a large density of states at the edge near Fermi level. The electronic properties of graphene [13] defined by their quasi-one-dimensional electronic confinement and the shape of the ribbon ends [14], indicates remarkable applications in graphene-based devices [15]. Graphene has similarities with many properties of CNT [10]. However, due to their planner structure, some of the properties seem to be easier to manipulate than CNTs. Being one atom thick, graphene comes in direct contact with substrate, thus interface state should play important role in sensing. Building and designing such nano-sensors that is able to make measurements of external deposited agents with ultrahigh resolution [16,17] is one of the main goals in the field of nanomechanics and is the topic of this paper.

Resonance based sensors [18–21] offer significant potential of achieving the high-fidelity requirement of many sensing applications. The principle of mass detection using resonators is based on the fact that the resonant frequency is sensitive to the resonator mass. The resonator mass includes the self-mass of the resonator and the attached mass. The change of the attached mass on the resonator causes a shift to the resonant frequency. The key issue of mass detection is in quantifying the change in the resonant frequency due to the added mass. In this article, we derive the calibration constants necessary for using single layer graphene sheet (SLGS) as a nanomechanical resonators in nanosized mass sensors. Natural vibration of SLGS with bio-fragment is discussed in Section 2. Four types of mass loadings are considered and closed-form equations have been derived for the frequency shift due to the added mass. Sensor equations and sensitivity calculations are discussed in Section 3. A molecular mechanics approach based on the universal force field (UFF) model [22,23] is used in Section 4 to validate the new results derived in the paper.

* Corresponding author. Tel.: +44 1792 602969; fax: +44 1792 295676.
E-mail addresses: S.Adhikari@swansea.ac.uk (S. Adhikari), R.Chowdhury@swansea.ac.uk, crajib2003@gmail.com (R. Chowdhury).

1386-9477/$ - see front matter © 2012 Elsevier B.V. All rights reserved.
http://dx.doi.org/10.1016/j.physe.2012.03.021

The results obtained using the analytical approach are discussed for three cases of mass distributions.

2. Natural vibration of SLGS with bio-fragment

The vibration of single and multiple layer graphene sheets has been investigated by several authors, using either continuum mechanics approaches [24], equivalent lattice structures made by atomistic-continuum models representing the C–C bonds [25], and molecular dynamics approaches combined with continuum mechanics for thickness identification [26]. The out-of-plane deformation of SLGS has been considered using the continuum mechanics models [24,27], together with continuum and truss-like structural assemblies [28–32].

Among the number of previous works, we consider the thin elastic plate model [24] for vibration analysis of single layer graphene sheets due to its simplicity. The equation of motion of the transverse free vibration of a thin elastic plate [33,34] of dimension $a \times b$ can be expressed as

$$D\left(\frac{\partial^4 u}{\partial x^4}+2\frac{\partial^2 u}{\partial x^2}\frac{\partial^2 u}{\partial y^2}+\frac{\partial^4 u}{\partial y^4}\right)+\rho\frac{\partial^2 u}{\partial t^2}=0, \quad 0\le x\le a,\ 0\le y\le b \tag{1}$$

Here $u \equiv u(x,y,t)$ is the transverse deflection, x and y are coordinates, t is the time, ρ is the mass density per area and the bending rigidity is defined by

$$D=\frac{Eh^3}{12(1-\nu^2)} \tag{2}$$

E is the Young's modulus, h is the thickness and ν is the Poisson's ratio. We consider rectangular graphene sheets with cantilevered (clamped at one edge) boundary condition.

2.1. Vibration of SLGS without attached mass

We first calculate the natural frequency of vibration of SLGS without any attached masses in order to obtain the frequency shift. Cantilever boundary condition is considered in this study. We are primarily interested in the first vibration mode of the system. Following Blevins [35], the first natural frequency (in rad/s) of a rectangular plate of dimension $a \times b$ can be expressed as

$$\omega_0^2=\left(\frac{\pi^4 D}{a^4\rho}\right)\frac{0.0313}{0.2268} \tag{3}$$

The above result, and in the subsequent analysis, it is assumed that the graphene sheets are in perfect planar configuration. However, spontaneous ripples and wrinkling have been identified by Meyer et al. [36] on free-standing graphene sheets through vacuum between metal struts. Edge stress induced warping and instability has been investigated using analytical [37], first principles study [38] and numerical methods [39]. Since the SLGS considered here is clamped at one edge, the substrate at the clamping edge may contain atomistic-scale defects resulting wrinkles along that edge. Inaccuracies arising due to the wrinkling of SLGS have been neglected in this paper. The vibration mode-shape for the first mode of vibration of the planar SLGS is given by

$$w(x,y)=1-\cos(\pi x/2a) \tag{4}$$

The natural frequency of the system can be alternatively obtained using the energy principle. Assuming the harmonic motion, the kinetic energy of the vibrating plate can be expressed by

$$T=\omega^2\int_A w^2(x,y)\rho\,\mathrm{d}A \tag{5}$$

Here ω denotes the frequency of oscillation and A denotes the area of the plate. Using the expression of $w(x,y)$ in Eq. (4) we have

$$T=\frac{1}{2}\omega^2\rho\int_0^a\int_0^b(1-\cos(\pi x/2a))^2\,\mathrm{d}x\,\mathrm{d}y = \frac{1}{2}\omega^2(ab\rho)\frac{3\pi-8}{2\pi} \tag{6}$$

The potential energy can be obtained as

$$U=\frac{D}{2}\int_A\left\{\left(\frac{\partial^2 w}{\partial x^2}+\frac{\partial^2 w}{\partial y^2}\right)^2-2(1-\nu)\left[\frac{\partial^2 w}{\partial x^2}\frac{\partial^2 w}{\partial y^2}-\left(\frac{\partial^2 w}{\partial x\partial y}\right)^2\right]\right\}\mathrm{d}A \tag{7}$$

Using the expression of $w(x,y)$ in Eq. (4) we have

$$U=\frac{D}{2}\rho\int_0^a\int_0^b\left(\frac{\partial^2 w}{\partial x^2}\right)^2\mathrm{d}x\,\mathrm{d}y=\frac{1}{2}\frac{\pi^4 D}{a^3}b(1/32) \tag{8}$$

Considering the energy balance, that is $T_{\max}=U_{\max}$, from Eqs. (6) and (8) the resonance frequency can be obtained as

$$\omega_0^2=\left(\frac{\pi^4 D}{a^4\rho}\right)\frac{1/32}{(3\pi-8)/2\pi} \tag{9}$$

This matches well with the numerical value reported in Eq. (3). Next, we calculate the kinetic energy due to additional attached mass and use the energy principle to obtain the modified resonance frequency.

2.2. Vibration of SLGS with attached mass

Several predominantly one-dimensional systems such as carbon nanotubes [40,41], and boron nitride nanotubes [42] have been used as nanomechanical resonator for mass sensing. Due to the two-dimensional nature of the graphene sheet, the SLGS resonator offers more flexibility in terms of attaching different types of molecules at different spatial locations. By exploiting the spatial spread of a graphene sheet, SLGS sensors can be designed such that it can effectively replace an array of cantilever sensors based on nanotubes only. A two-dimensional surface offers huge opportunities for attaching molecules to the graphene sheet.

We consider four possible arrangements by which bio-molecules can be attached with the graphene sheet. The four cases considered here are

- Case (a): masses at the cantilever tip in a line.
- Case (b): masses in a line along the width.
- Case (c): masses in a line along the length.
- Case (d): masses in a line with an arbitrary angle.

Pictorial representations of these four cases are shown in Fig. 1. It is certainly possible to have different mass distributions other than the four considered here. The method developed in this paper is general and can be applied to more general cases if the geometry is known. The reason behind the selection of the four cases in Fig. 1 is to develop an understanding on the behaviour of the proposed sensor for typical mass distributions.

From the practical point of view, for label-free sensors it is generally not possible to a priori know exactly the spatial location of the attached molecules [40]. High resolution imaging techniques can be used to capture the spatial location of the attached molecules. Alternatively, many nanomechanical biosensors use specific coatings on the resonators to make them sensitive to particular biomolecules. In this approach, the sensor will not be label-free but the spatial location of the attachment region will be a priori known. The attachment region can even be optimally designed taking the shape and size of the molecules to be

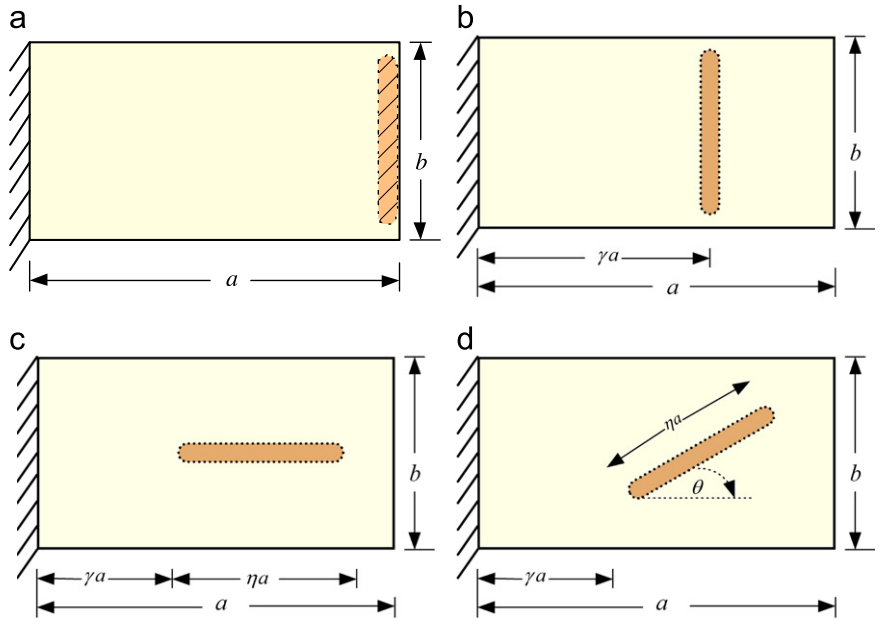

Fig. 1. Configurations of attached masses in a cantilevered SLGS resonator. (a) Masses at the cantilever tip in a line; (b) masses in a line along the width; (c) masses in a line along the length; and (d) masses in a line with an arbitrary angle.

detected in to account. The analysis presented below is valid for both of these approaches. The analytical results to be derived precisely quantify the effect of spatial location of the attached molecules (not just their mass) on the performance of the sensor.

We first consider the case when the attached masses are at the cantilever tip in a line as shown in Fig. 1(a). Assuming the total attached mass is M, the combined kinetic energy of the SLGS and the attached mass can be obtained as

$$T_a = \frac{1}{2}\omega^2\left\{\int_A w^2(x,y)\rho\ \mathrm{d}A + Mw^2(x,y)\Big|_{x=a}\right\} = \frac{1}{2}\omega^2\left\{M_g\frac{3\pi-8}{2\pi}+M\right\} \tag{10}$$

where

$$M_g = \rho ab \tag{11}$$

is the mass of the graphene sheet. Considering the energy balance, that is $T_{\max} = U_{\max}$, from Eqs. (8) and (10) the resonance frequency can be obtained as

$$\omega_a^2 = \frac{\frac{1}{2}\frac{\pi^4 D}{a^3}b(1/32)}{\frac{1}{2}\left\{ab\rho\frac{3\pi-8}{2\pi}+M\right\}} = \left(\frac{\pi^4 D}{a^4\rho}\right)\frac{1/32}{(3\pi-8)/2\pi+M/M_g} \tag{12}$$

This equation shows how the added mass M reduces the resonance frequency.

Next we consider the case when the attached masses are arranged in a line along the width as shown in Fig. 1(b). It is assumed that the masses are at a distance of γa, $\gamma \le 1$, from the fixed edge of the graphene sheet. The kinetic energy of the system can be obtained as

$$T_b = \frac{1}{2}\omega^2\left\{\int_A w^2(x,y)\rho\ \mathrm{d}A + Mw^2(x,y)\Big|_{x=\gamma a}\right\} = \frac{1}{2}\omega^2\left\{M_g\frac{3\pi-8}{2\pi}+M\alpha_b\right\} \tag{13}$$

where the factor

$$\alpha_b = (1-\cos(\pi\gamma/2))^2 \tag{14}$$

For the case shown in Fig. 1(c), we assume that the length of the attached mass is ηa and its density along the length is uniform. We also consider that the mass is placed at a distance of γa from the fixed edge. Since the mass always remains within the graphene sheet, both $\gamma \le 1$, $\eta \le 1$ and additionally $\gamma+\eta \le 1$. The kinetic energy of the system can be obtained as

$$T_c = \frac{1}{2}\omega^2\left\{\int_A w^2(x,y)\rho\ \mathrm{d}A + \int_{\gamma a}^{(\gamma+\eta)a}\frac{M}{\eta a}w^2(x,y)\ \mathrm{d}x\right\} = \frac{1}{2}\omega^2\left\{M_g\frac{3\pi-8}{2\pi}+M\alpha_c\right\} \tag{15}$$

where by calculating the above integral one has

$$\alpha_c = \frac{3\pi\eta+[\sin((\gamma+\eta)\pi)-\sin(\gamma\pi)]-8[\sin((\gamma+\eta)\pi/2)-\sin(\gamma\pi/2)]}{2\pi\eta} \tag{16}$$

In the above expression we use $M/\eta a$ as the mass per unit length of the attached object. The most general case of the attached object is shown in Fig. 1(d). Depending on the value of θ, it reduces to the two previous cases. The values of γ and η should be such that the mass remains within the graphene sheet. This implies that $\gamma+\eta\cos(\theta) \le 1$ and $\eta a \le b\csc(\theta)$. Considering the mass per unit length along the x-axis as $M/\eta a\cos(\theta)$, the kinetic energy of the system can be obtained as

$$T_d = \frac{1}{2}\omega^2\left\{\int_A w^2(x,y)\rho\ \mathrm{d}A + \int_{\gamma a}^{(\gamma+\eta\cos(\theta))a}\frac{M}{\eta a\cos(\theta)}w^2(x,y)\ \mathrm{d}x\right\} = \frac{1}{2}\omega^2\left\{M_g\frac{3\pi-8}{2\pi}+M\alpha_c\right\} \tag{17}$$

where

$$\alpha_d = \frac{3\pi\eta\cos(\theta)+[\sin((\gamma+\eta\cos(\theta))\pi)-\sin(\gamma\pi)]-8[\sin((\gamma+\eta\cos(\theta))\pi/2)-\sin(\gamma\pi/2)]}{2\pi\eta\cos(\theta)} \tag{18}$$

Taking the limit $\theta\to\pi/2$ and $\theta\to 0$, Eq. (17) reduces to Eqs. (13) and (15), respectively.

The resonance frequency corresponding to cases (b)–(d) can be obtained using the energy principle used for case (a). Considering the energy balance, the resonance frequency can be expressed in a

general form as

$$\omega_{b,c,d}^2 = \frac{\frac{1}{2}\frac{\pi^4 D}{a^3} b(1/32)}{\frac{1}{2}\left\{ab\rho\frac{3\pi-8}{2\pi}+\alpha_{b,c,d}M\right\}} = \left(\frac{\pi^4 D}{a^4\rho}\right)\frac{1/32}{(3\pi-8)/2\pi+\mu\alpha_{b,c,d}} \tag{19}$$

Here the ratio of the added mass

$$\mu = \frac{M}{M_g} \tag{20}$$

and $\alpha_{b,c,d}$ are factors which depend on the mass distribution as defined before.

3. Sensor equations and sensitivity analysis

For notational convenience, we express the natural frequency of the mass loaded graphene sheet as

$$\omega_n^2 = \left(\frac{\pi^4 D}{a^4\rho}\right)\frac{1/32}{(3\pi-8)/2\pi+\mu\alpha_n} \tag{21}$$

where α_n stands for different values of α, which in turn depend on the distribution of the attached mass.

Taking the ratio with the resonance frequency of the graphene sheet without any mass in Eq. (9), we have

$$\frac{\omega_n}{\omega_0} = \frac{1}{\sqrt{1+c_n\mu}} \tag{22}$$

Here the calibration constant c_n is given by

$$c_n = \frac{2\pi\alpha_n}{3\pi-8} \tag{23}$$

The calibration constants for the four different cases considered here is summarised in Table 1. Considering $\omega = 2\pi f$, the frequency shift in Hz due to the added mass can be obtained as

$$\Delta f = f_0 - f_n = 2\pi(\omega_0-\omega_n) \tag{24}$$

The relative frequency shift [18,20] can be obtained from Eq. (24) as

$$\frac{\Delta f}{f_0} = 1-\frac{1}{\sqrt{1+c_n\mu}} \tag{25}$$

Using this expression, the relative added mass of the bio-fragment can be obtained from the frequency shift as

$$\mu = \frac{1}{c_n\left(1-\frac{\Delta f}{f_0}\right)^2}-\frac{1}{c_n} \tag{26}$$

The normalised sensitivity of the graphene based sensor can be obtained by the differentiation of Eq. (25) as

$$\frac{\partial\left(\frac{\Delta f}{f_0}\right)}{\partial\mu} = \frac{c_n}{2(1+c_n\mu)^{3/2}} \approx \frac{c_n}{2}(1-(3/2)(c_n\mu) +(15/8)(c_n\mu)^2-(35/16)(c_n\mu)^3+\cdots) \tag{27}$$

The dimensional sensitivity (in Hz/g) can be obtained from Eq. (27) as

$$\frac{\partial(\Delta f)}{\partial M} = \frac{f_0}{M_g}\frac{c_n}{2}(1+c_n\mu)^{-3/2} \tag{28}$$

The absolute maximum sensitivity of a grapheme based sensor therefore given by

$$\left.\frac{\partial(\Delta f)}{\partial M}\right|_{\max} = \frac{f_0}{M_g}\frac{c_n}{2} \tag{29}$$

This implies that for a given graphene sheet, the higher value of c_n will result in a sensor with higher sensitivity. The four calibration constants given in Table 1 are plotted for different values of the normalised length η in Fig. 2. It can be seen that, among the four cases considered here, case (a), that is, when the masses are at the cantilever tip is the most sensitive case since the value of the calibration constant is the highest for this case. Therefore, for graphene based sensors in the cantilever configuration, it is desirable to place the mass at the free edge.

4. Analysis of numerical results

In this section we validate the sensor equations derived in Section 3 based on the frequency shift. We use armchair single layer graphene sheet of length 4.12 nm and width 2.21 nm. The mass of the SLGS is 7.57 zg (1 zg = 10^{-21} g) and in the cantilever configuration its first natural frequency is 23.96 GHz. The added bio-fragment is considered to be adenosine, which is a nucleoside composed of a molecule of adenine attached to a ribose sugar molecule. Adenosine plays an important role in biochemical

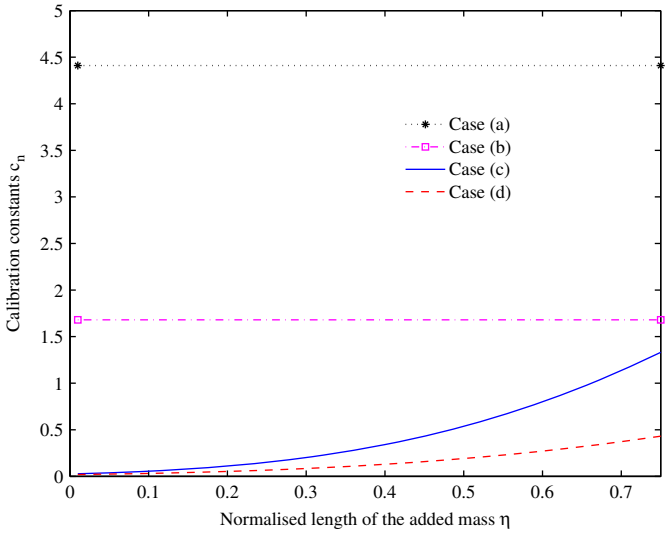

Fig. 2. Calibration constants corresponding to four cases. Case (a) is independent of γ and η. For case (b), the value of $\gamma = 0.75$ is considered. For case (c), the value of $\gamma = 0.25$ and the normalised length η is varied between 0 and 0.75. For case (d), the value of angle $\theta = \pi/4$ and rest of the values are kept same as case (c).

Table 1
The calibration constants for SLGS based bio-nanosensor due to four possible configurations of attached mass.

Mass arrangement	Calibration constant c_n
Case (a): masses are at the cantilever tip in a line	$2\pi/(3\pi-8)$
Case (b): masses are in a line along the width	$2\pi(1-\cos(\pi\gamma/2))^2/(3\pi-8)$
Case (c): masses are in a line along the length	$(3\pi\eta+[\sin((\gamma+\eta)\pi)-\sin(\gamma\pi)]-8[\sin((\gamma+\eta)\pi/2)-\sin(\gamma\pi/2)])/\eta(3\pi-8)$
Case (d): masses are in a line with an arbitrary angle θ	$(3\pi\eta\cos(\theta)+[\sin((\gamma+\eta\cos(\theta))\pi)-\sin(\gamma\pi)]-8[\sin((\gamma+\eta\cos(\theta))\pi/2)-\sin(\gamma\pi/2)])/\eta\cos(\theta)(3\pi-8)$

processes, such as energy transfer as adenosine triphosphate (ATP) and adenosine diphosphate (ADP) as well as in signal transduction as cyclic adenosine monophosphate. It is also an inhibitory neurotransmitter, believed to play a role in promoting sleep and suppressing arousal, with levels increasing with each hour an organism is awake. Here we investigate the possibility of detecting Adenosine using a cantilevered single layer graphene sheet. The mass of each adenosine molecule is 0.44 zg, which is about 6% of the graphene mass.

The added mass and the corresponding frequency-shift are calculated from the molecular mechanics approach. The molecular mechanics approach used here [43] is more accurate compared to the atomistic finite element method [31,32]. We used the Gaussian software [44] in conjunction with the UFF model developed by Rappe et al. [22]. The calculation of frequency and their validation for CNTs were given in Ref. [45]. A detailed study on transverse vibration of single layer graphene sheets using the methodology adopted is illustrated in Ref. [43]. The general expression of total energy is a sum of energies due to valence or bonded interactions and non-bonded interactions [22]

$$E=\sum_{0}^{N_B}\frac{1}{2}k_{IJ}(r-r_{IJ})^2+\sum_{0}^{N_A}k_{IJK}(C_0+C_1\cos\theta+C_2\cos 2\theta)+\sum_{0}^{N_T}\frac{1}{2}V_\phi(1-\cos(n\phi_0)\cos(n\phi))+\sum_{0}^{N_I}V_\omega(C_0^I+C_1^I\cos\omega+C_2^I\cos 2\omega)+\sum_{0}^{N_{nb}}R_{IJ}\left[-2\left(\frac{x_{IJ}}{x}\right)^6+\left(\frac{x_{IJ}}{x}\right)^{12}\right]+\sum_{0}^{N_{nb}}\frac{q_I\cdot q_J}{\varepsilon\cdot x} \quad (30)$$

In the above equation N_B, N_A, N_T, N_I and N_{nb} are the numbers of the bond-, angle-, torsion-, inversion- and the non-bonded-terms, respectively. The constants k_{IJ} and k_{IJK} are the force constants of the bond- and angle-terms, respectively. r and r_{IJ} are the bond distance and natural bond distance of the two atoms I and J, respectively. θ and θ_0 are the angle and natural angle for three atoms I–J–K, respectively. ϕ and ϕ_0 are the torsion angle and torsion natural angle for three atoms I–J–K–L, respectively. V_ϕ, n, V_ω, and ω are the height of the torsion barrier, periodicity of the torsion potential, height of the inversion barrier and inversion- or out-of-plane-angle at atom I, respectively. C_0^I, C_1^I and C_2^I are the Fourier coefficients of the inversions terms. x and x_{IJ} are the distance and natural distance of two non-bonded atoms I and J. R_{IJ} is the depth of the Lennard–Jones potential. q_I and ε are the partial charge of atoms I and dielectric constant. For the general non-linear case, the bend function should have a minimum $\theta=\theta_0$, with the second derivative at θ_0 equal to the force constant (k_{IJK}). The Fourier coefficients of the general angle terms C_0, C_1 and C_2 are evaluated as a function of the natural angle θ_0 as $C_2=1/4\sin^2\theta_0$, $C_1=-4C_2\cos\theta_0$ and $C_0=C_2(2\cos^2\theta_0+1)$. The bond stretching force constants (k_{IJ}) are atom based and are obtained from generalisation of Badger's rules. The assumption is that the bonding is dominated by attractive ionic terms plus short-range Pauli repulsions [22]. The force constant (in units of (kcal/mol)/A^2) then becomes

$$k_{IJ}=644.12\frac{Z_I^*Z_J^*}{r_{IJ}^3} \quad (31)$$

The Z_I^* is the effective atomic charges, in electron units. Similarly, the angle bend force constants (k_{IJK}) are generated using the angular generalisation of Badger's rule. The force constant (in units of kcal/mol rad^2) then becomes [44]

$$k_{IJK}=644.12\frac{Z_I^*Z_J^*}{r_{IJ}^5}[3r_{IJ}r_{JK}(1-\cos^2\theta_0)-r_{IK}^2\cos\theta_0] \quad (32)$$

The torsional constant (kcal/mol) is defined as

$$V_\phi=5\sqrt{U_IU_J}[1+4.18\ln(BO_{JK})] \quad (33)$$

where, BO_{JK} is the bond order for Atom-J and Atom-K. U_I and U_J are the atomic constants defined with UFF sp^2. Regarding the inversion term, the coefficients are $C_0^I=1$, $C_1^I=-1$ and $C_2^I=0$ for sp^2 atom type. The frequencies are calculated using the Hessian of the total energy E in Eq. (30) as implemented in Gaussian [44].

Here we calculate the natural frequency of the bare graphene sheet and graphene sheet with attached bio fragments. From these two sets of frequencies, the frequency shifts are calculated. These frequency shifts in turn are considered as experimental observations and used in the sensor Eq. (26). The value of the mass predicted by this equation are then compared with the known values used in the molecular mechanics simulations. The analytical approach is verified with the exact approach in Fig. 3 for case (a) when the added molecules are at the cantilever tip in a line. It can be seen that the results from the energy based analytical approach match the exact results obtained from the molecular mechanics reasonably well. The maximum sensitivity

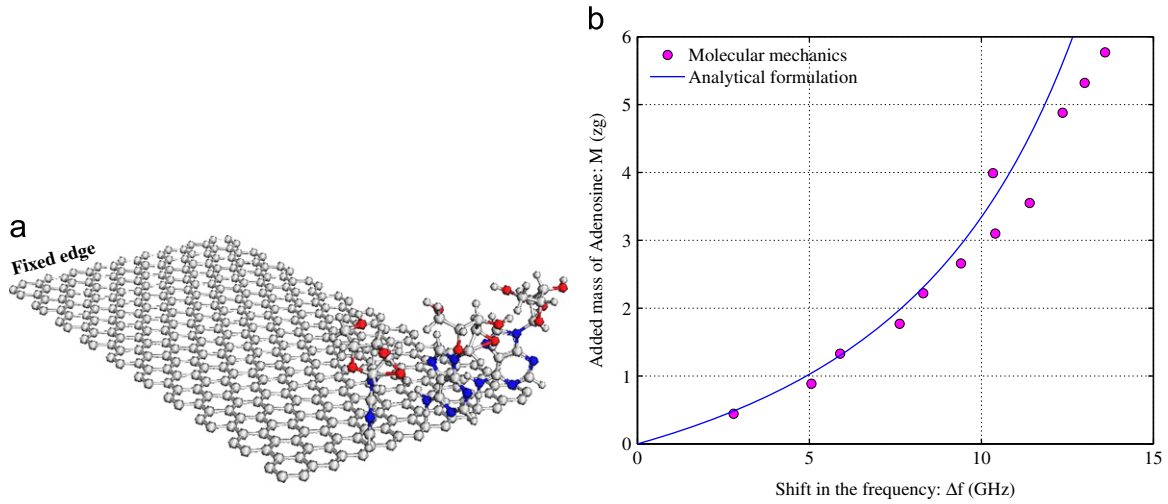

Fig. 3. Identified attached masses from the frequency-shift of a cantilevered SLGS resonator for case (a). The SLGS mass is 7.57 zg and the mass of each adenosine molecule is 0.44 zg. The proposed approach is validated using data from the molecular mechanics simulations. Up to 12 adenosine molecules are attached to the graphene sheet. (a) SLGS with adenosine molecules at the cantilever tip in a line and (b) identified mass from the frequency shift.

obtained from Eq. (29) is calculated as 6.9761 GHz/zg. When the added mass is very high (when mass ratio is more than 0.3), the proposed analytical approach becomes less accurate. This is expected as for such high value of the added mass, the assumed deformation shape in Eq. (4) is not strictly applicable as it was derived for SLGS without any added mass. As a consequence the energy expressions and consequence the frequency estimate becomes inaccurate. This analysis showed that the proposed expressions are accurate up to added mass weighing 35% of the SLGS mass. Beyond this the proposed approach starts to lose accuracy. This is however is not a severe limitation as 35% of the SLGS mass can be adequate for practical applications. If higher mass needs to be identified, one can simply use a larger SLGS within the sensor device. We therefore conclude that the mass of SLGS should be approximately more than 3 times the mass to be detected in order to reliably use the proposed analytical expressions.

Fig. 4 shows the identified masses from the frequency-shift for case (b), that is, when the added adenosine molecules are arranged in a line along the width. For the analytical calculation we use $\gamma = 0.85$. The maximum sensitivity obtained from Eq. (29) is calculated as 4.0992 GHz/zg. It can be seen that, except few cases, the results from the energy based analytical approach match the exact results obtained from the molecular mechanics reasonably well. Compared to the previous case it can also be seen that for a given value of added mass, the relative frequency shift is less for this case. This implies that the SLGS based sensor for this mass distribution is less sensitive compared to the case when the mass was placed at the edge.

Identified masses corresponding to case (d) is shown in Fig. 5. This is the most general case when the added masses are arranged in a line with an arbitrary angle. Case (c) is not shown as it is a special case of case (d). For the results shown in Fig. 5, we consider $\gamma = 0.25$, $\eta = 0.7$ and $\theta = \pi/6$. The maximum sensitivity obtained from Eq. (29) is calculated as 1.7401 GHz/zg. The proposed approach generally captures the trend of the added mass but the accuracy is lower compared to the last two cases. This can be explained from the fact the sensitivity is the lowest for this case.

5. Conclusions

In this theoretical study, we investigated the possibility of using single layer graphene sheet (SLGS) as a nanoscale label-free

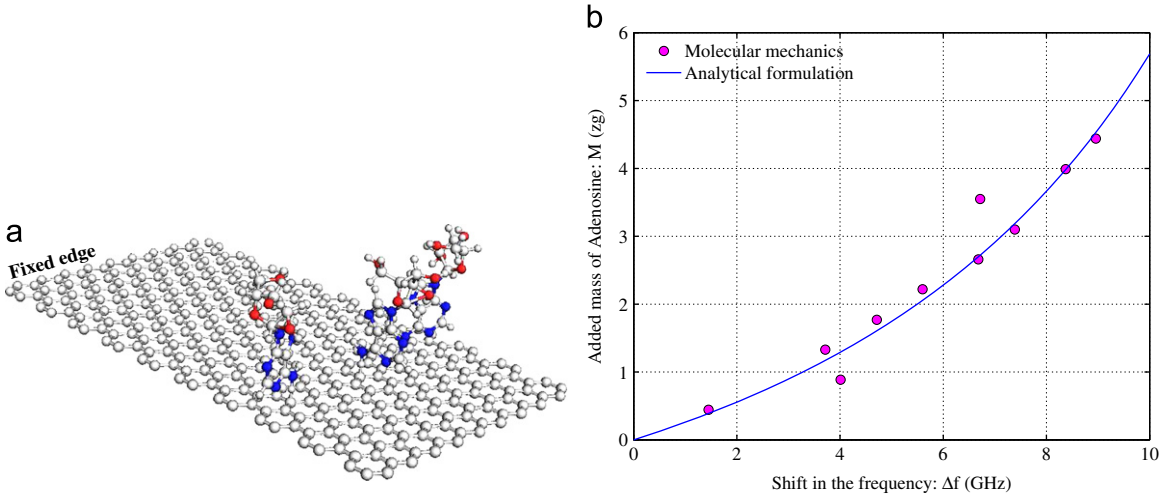

Fig. 4. Identified attached masses from the frequency-shift of a cantilevered SLGS resonator for case (b). The proposed approach is validated using data from the molecular mechanics simulations. Up to 10 adenosine molecules are attached to the graphene sheet. (a) SLGS with adenosine molecules in a line along the width and (b) identified mass from the frequency shift, $\gamma = 0.85$.

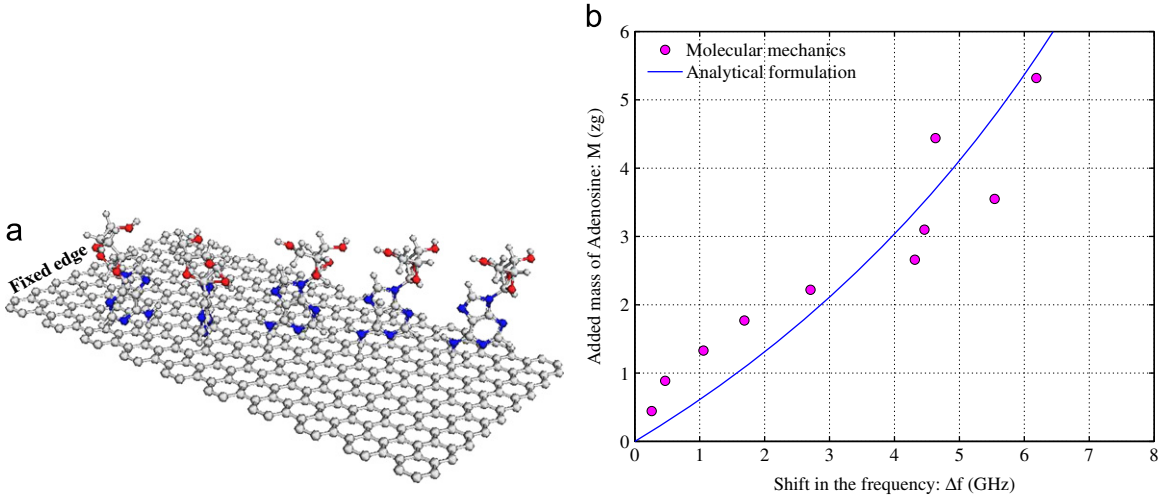

Fig. 5. Identified attached masses from the frequency-shift of a cantilevered SLGS resonator for case (d). The proposed approach is validated using data from the molecular mechanics simulations. Up to 10 adenosine molecules are attached to the graphene sheet. (a) SLGS with adenosine molecules in a line with an arbitrary angle and (b) identified mass from the frequency shift, $\gamma = 0.25$, $\eta = 0.7$ and $\theta = \pi/6$.

mass sensor. The shift in the resonance frequencies due to the additional mass is exploited in the proposed sensor. We observe that the performance of the sensor depends on the spatial distribution of the attached mass on the graphene sheet. The SLGS resonator is assumed to be in cantilevered configuration. Four physically realistic mass distributions are considered. These include masses at the cantilever tip in a line, masses in a line along the width, masses in a line along the length and masses in a line with an arbitrary angle. Explicit closed-form analytical expressions have been derived to detect the added mass from the frequency shift. Sensitivities of the proposed sensor for different mass distributions are compared. A molecular mechanics based approach is used to validate the analytical sensor equations. We used the UFF force field model, wherein the force field parameters are estimated using the general rules based on the element, its hybridisation and its connectivity. Acceptable agreements between the proposed approach and the molecular mechanics simulations have been observed. Numerical results indicate that the new equations derived in the paper are acceptable when the added mass is up to 1/3 of the mass of the SLGS cantilever. Our analysis show that by placing the bio-molecules at the edge of the graphene sheet results in the most sensitive sensor. Further research will include the dynamics of the subgrade which is essential for immobilising the bio-molecules on to the graphene sheets. Significant work is also necessary to physically realise a graphene based mass sensing resonator where the analytical expressions developed in this paper would be utilised.

Acknowledgments

SA and RC acknowledge the support of Royal Society through the award of Wolfson Research Merit award and Newton International Fellowship, respectively.

References

[1] M. Pumera, A. Ambrosi, A. Bonanni, E.L.K. Chng, H.L. Poh, Trends in Analytical Chemistry 29 (9) (2010) 954.
[2] B. Huang, Z. Li, Z. Liu, G. Zhou, S. Hao, J. Wu, B.-L. Gu, W. Duan, Journal of Physical Chemistry C 112 (35) (2008) 13442.
[3] Y. Shao, J. Wang, H. Wu, J. Liu, I.A. Aksay, Y. Lin, Electroanalysis 22 (10) (2010) 1027.
[4] P.K. Ang, W. Chen, A.T.S. Wee, K.P. Loh, Journal of the American Chemical Society 130 (44) (2008) 14392+.
[5] N. Mohanty, V. Berry, Nano Letters 8 (12) (2008) 4469.
[6] R. Arsat, M. Breedon, M. Shafiei, P.G. Spizziri, S. Gilje, R.B. Kaner, K. Kalantar-Zadeh, W. Wlodarski, Chemical Physics Letters 467 (4–6) (2009) 344.
[7] M. Qazi, G. Koley, Sensors 8 (11) (2008) 7144.
[8] S.S. Yu, W.T. Zheng, Q. Jiang, IEEE Transactions on Nanotechnology 7 (5) (2008) 628.
[9] R. Moradian, Y. Mohammadi, N. Ghobadi, Investigation of gas sensing properties of armchair graphene nanoribbons, Journal of Physics: Condensed Matter 20 (42) (2008).
[10] D.V. Kosynkin, A.L. Higginbotham, A. Sinitskii, J.R. Lomeda, A. Dimiev, B.K. Price, J.M. Tour, Nature 458 (7240) (2009) 872.
[11] A. Hirsch, Angewandte Chemie-International Edition 48 (36) (2009) 6594.
[12] B. Biel, X. Blase, F. Triozon, S. Roche, Anomalous doping effects on charge transport in graphene nanoribbons, Physical Review Letters 102 (9) (2009).
[13] R. Chowdhury, S. Adhikari, P. Rees, F. Scarpa, S.P. Wilks, Graphene-based biosensor using transport properties, Physical Review B 83 (4) (2011) 045401-1–045401-8.
[14] L. Rosales, M. Pacheco, Z. Barticevic, A. Latge, P.A. Orellana, Transport properties of graphene nanoribbons with side-attached organic molecules, Nanotechnology 19 (6) (2008).
[15] H. Santos, L. Chico, L. Brey, Carbon nanoelectronics: unzipping tubes into graphene ribbons, Physical Review Letters 103 (8) (2009).
[16] L.-C. Jiang, W.-D. Zhang, Biosensors & Bioelectronics 25 (6) (2010) 1402.
[17] Y. Li, X. Qiu, F. Yang, X.-S. Wang, Y. Yin, Ultra-high sensitivity of super carbon-nanotube-based mass and strain sensors, Nanotechnology 19 (16) (2008).
[18] R. Chowdhury, S. Adhikari, J. Mitchell, Physica E: Low-Dimensional Systems and Nanostructures 42 (2) (2009) 104.
[19] C.Y. Li, T.W. Chou, Applied Physics Letters 84 (25) (2004) 5246.
[20] S. Adhikari, R. Chowdhury, Journal of Applied Physics 107 (12) (2010) 124322:1.
[21] A.Y. Joshi, S.C. Sharma, S.P. Harsha, Sensors and Actuators A: Physical 168 (2) (2011) 275.
[22] A.K. Rappe, C.J. Casewit, K.S. Colwell, W.A. Goddard, W.M. Skiff, Journal of the American Chemical Society 114 (25) (1992) 10024.
[23] R. Chowdhury, S. Adhikari, F. Scarpa, Applied Physics A 102 (2) (2011) 301.
[24] S. Kitipornchai, X.Q. He, K.M. Liew, Physical Review B 72 (7) (2005) 075443 1.
[25] K. Hashemnia, M. Farid, R. Vatankhah, Computational Materials Science 47 (1) (2009) 79.
[26] S.S. Gupta, R.C. Batra, Journal of Computational and Theoretical Nanoscience 7 (10) (2010) 2151.
[27] W.H. Duan, C.M. Wang, Nanotechnology 20 (2009) 075702.
[28] G.M. Odegard, T.S. Gates, L.M. Nicholson, K.E. Wise, Composites Science and Technology 62 (14) (2002) 1869.
[29] R. Chowdhury, C.Y. Wang, S. Adhikari, Journal of Physics D: Applied Physics 43 (8) (2010) 085405.
[30] K.I. Tserpes, P. Papanikos, Composites Part B 36 (2005) 468.
[31] F. Scarpa, S. Adhikari, Journal of Physics D: Applied Physics 41 (085306) (2008) 1.
[32] F. Scarpa, S. Adhikari, A.J. Gil, C. Remillat, Nanotechnology 20 (12) (2010) 085405.
[33] S. Timoshenko, Theory of Plates and Shells, McGraw-Hill Inc., New York, 1940.
[34] W. Soedel, Vibrations of Shells and Plates, third ed., Marcel Dekker Inc, New York, 2004.
[35] R.D. Blevins, Formulas for Natural Frequency and Mode Shape, Krieger Publishing Company, Malabar, FL, USA, 1984.
[36] J.C. Meyer, A.K. Geim, M.I. Katsnelson, K.S. Novoselov, T.J. Booth, S. Roth, Nature 446 (2007) 60.
[37] V.B. Shenoy, C.D. Reddy, A. Ramasubramaniam, Y. Zhang, Physical Review Letters 101 (245501) (2008) 1.
[38] B. Huang, M. Liu, N. Su, J. Wu, W. Duan, B. lin Gu, F. Liu, Physical Review Letters 102 (166404) (2009) 1.
[39] A.J. Gil, S. Adhikari, F. Scarpa, J. Bonet, Journal of Physics: Condensed Matter 22 (14) (2010) 145302.
[40] A. Boisen, Nature Nanotechnology 4 (7) (2009) 404.
[41] H.B. Peng, C.W. Chang, S. Aloni, T.D. Yuzvinsky, A. Zettl, Physical Review Letters 97 (8) (2006) 087203.
[42] R. Chowdhury, S. Adhikari, IEEE Transactions on Nanotechnology 10 (4) (2011) 659.
[43] R. Chowdhury, S. Adhikari, F. Scarpa, M.I. Friswell, Journal of Physics D: Applied Physics 44 (20) (2011) 205401:1.
[44] M.J. Frisch, G.W. Trucks, H.B. Schlegel, G.E. Scuseria, M.A. Robb, J.R. Cheeseman, G. Scalmani, V. Barone, B. Mennucci, G.A. Petersson, H. Nakatsuji, M. Caricato, X. Li, H.P. Hratchian, A.F. Izmaylov, J. Bloino, G. Zheng, J.L. Sonnenberg, M. Hada, M. Ehara, K. Toyota, R. Fukuda, J. Hasegawa, M. Ishida, T. Nakajima, Y. Honda, O. Kitao, H. Nakai, T. Vreven, J.A. Montgomery, Jr., J.E. Peralta, F. Ogliaro, M. Bearpark, J.J. Heyd, E. Brothers, K.N. Kudin, V.N. Staroverov, R. Kobayashi, J. Normand, K. Raghavachari, A. Rendell, J.C. Burant, S.S. Iyengar, J. Tomasi, M. Cossi, N. Rega, J.M. Millam, M. Klene, J.E. Knox, J.B. Cross, V. Bakken, C. Adamo, J. Jaramillo, R. Gomperts, R.E. Stratmann, O. Yazyev, A.J. Austin, R. Cammi, C. Pomelli, J.W. Ochterski, R.L. Martin, K. Morokuma, V.G. Zakrzewski, G.A. Voth, P. Salvador, J.J. Dannenberg, S. Dapprich, A.D. Daniels, O. Farkas, J.B. Foresman, J.V. Ortiz, J. Cioslowski, D.J. Fox, Gaussian 09 Revision A.1 (2009).
[45] R. Chowdhury, S. Adhikari, C.Y. Wang, F. Scarpa, Computational Materials Science 48 (4) (2010) 730.